

Expedited Articles

Comparative Molecular Field Analysis of Haptens Docked to the Multispecific Antibody IgE(Lb4)

Armin M. Gamper,^{†,‡} Rudolf H. Winger,[†] Klaus R. Liedl,[†] Christoph A. Sotriffer,[†] Janos M. Varga,[†] Romano T. Kroemer,[‡] and Bernd M. Rode*,[†]

Department of General, Inorganic and Theoretical Chemistry, University of Innsbruck, Innrain 52a, A-6020 Innsbruck, Austria, Department of Dermatology, University of Innsbruck, Anichstrasse 35, A-6020 Innsbruck, Austria, and Physical and Theoretical Chemistry Laboratory, University of Oxford, South Parks Road, Oxford OX1 3QZ, England, U.K.

Received March 25, 1996[®]

Using comparative molecular field analysis (CoMFA), three-dimensional quantitative structure–activity relationships were developed for 27 haptens which bind to the monoclonal antibody IgE(Lb4). In order to obtain an alignment for these structurally very diverse antigens, the compounds were docked to a previously modeled receptor structure using the automated docking program AUTODOCK (Goodsell, D. S.; Olson, A. J. *Proteins: Struct., Funct., Genet.* **1990**, *8*, 195–202). Remarkably, this alignment method yielded highly consistent QSAR models, as indicated by the corresponding cross-validated r^2 values (0.809 for a model with carbon as probe atom, 0.773 for a model with hydrogen as probe atom). Conventional alignment failed in providing a basis for self-consistent CoMFAs. Amino acids Tyr H 50, Tyr H 52, and Trp H 95 of the receptor appeared to be of crucial importance for binding of various antigens. These findings are consistent with earlier considerations of aromatic residues being responsible for the multispecificity of certain immunoglobulins.

Introduction

The concept of multispecific antibodies was first stated by Talmage¹ in 1959 and has since been extended further.^{2,3} In several studies of antibody specificity for monoclonal antibodies (mAbs), it has been noted that some mAbs have a broad binding specificity. The so-called heteroclitic antibodies showed an even higher affinity for ligands structurally different than the original ones.⁴ For example, some of the 13 IgE monoclonal antibodies in a library made to the hapten trinitrophenyl were able to bind dinitrophenyl (DNP) more strongly.^{5,6}

Two of the IgE clones (named La2 and Lb4) from this collection were examined and found to have a wide range of ligand binding specificities. Of the over 2000 investigated compounds, several ones showed high affinity although having no apparent structural similarity to DNP.⁷ An unusually high number of aromatic residues was found in the variable domains of these two IgE mAbs.⁸ In order to investigate these domains further, the structure of the variable region constituting the binding site of immunoglobulin Lb4 was generated by means of knowledge-based modeling techniques.⁹ In addition, the association constants for a variety of ligands were measured by absorption spectroscopy, and the nature of the ligand–receptor interaction was

explored by docking the haptens to the antibody model,¹⁰ using the program AUTODOCK.¹¹

Since it was not possible to correlate the computed docking energies with the experimentally determined association constants, we decided to perform a 3D-QSAR study based on the alignment of the docked ligands. Of special interest was the question whether an alignment of structurally highly diverse compounds, based on computational docking to a receptor, would lead to a consistent QSAR model. Furthermore, we were interested to find out whether we could identify residues of particular importance for binding of the ligand molecules.

The QSAR models were derived using the CoMFA approach.¹² Within CoMFA, steric and electrostatic interaction energies between a probe atom and a set of superimposed molecules are calculated at the surrounding points of a predefined grid. These energy values are subsequently correlated with some property of the compounds (such as biological activity). Linear equations are derived by means of the partial least squares (PLS) algorithm.^{13–15} The quality of the resulting QSAR models is indicated by the cross-validated r^2 value (r^2_{cv}).^{12,16} Very useful results of the CoMFA procedure are the three-dimensional coefficient contour maps which indicate regions of favorable steric and electrostatic interaction around the set of molecules.

The antigens investigated covered a very large property space, ranging from DNP-substituted amino acids to diaspurin, from negatively charged molecules such as hemimellitic acid to double positive protonium iodide (Table 1). Initial trials to superimpose these diverse molecules applying systematic conformational searches (using distance maps in an “active analogue approach”)¹⁷ or field-fitting approaches did not yield

* Author to whom all correspondence should be addressed. Tel: ++43-512-507-5160. Fax: ++43-512-507-2935. E-mail: Bernd.M.Rode@uibk.ac.at.

[†] University of Innsbruck, Innrain.

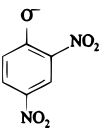
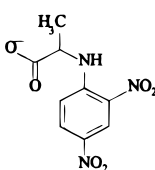
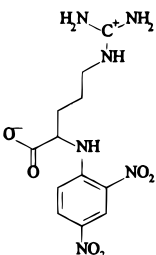
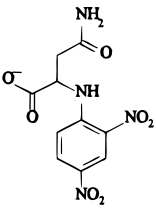
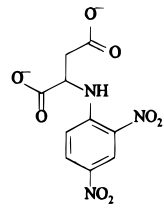
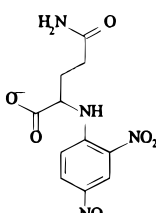
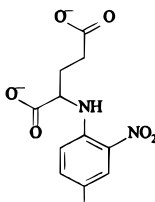
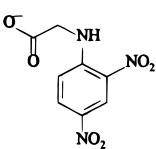
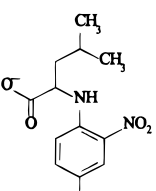
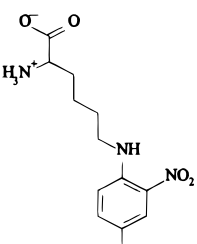
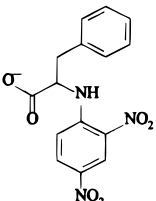
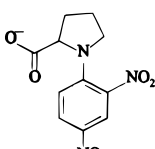
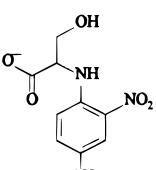
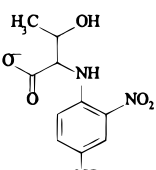
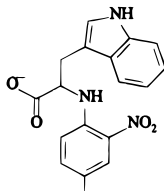
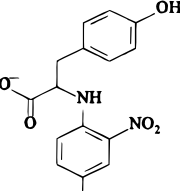
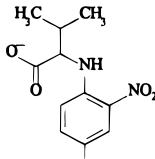
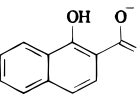
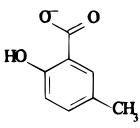
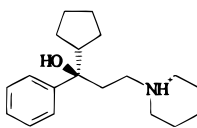
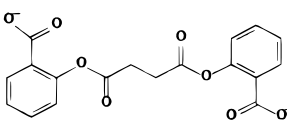
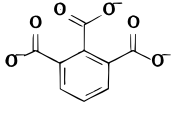
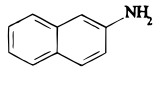
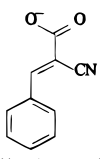
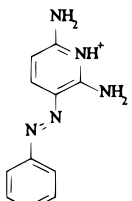
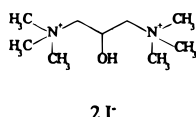
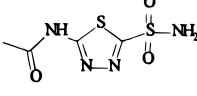
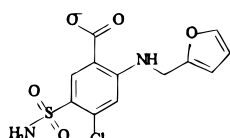
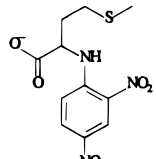
[‡] Current address: Department of Biochemistry, Free University of Berlin, Thielallee 63, 14195 Berlin (Dahlem), Germany.

[§] University of Innsbruck, Anichstrasse.

^{||} University of Oxford.

[®] Abstract published in *Advance ACS Abstracts*, August 15, 1996.

Table 1. Structures of the Haptens Investigated

| | | | | |
|---|---|--|---|---|
|  |  |  |  |  |
| 2,4-Dinitrophenolate | DNP-Ala | DNP-Arg | DNP-Asn | DNP-Asp |
|  |  |  |  |  |
| DNP-Gln | DNP-Glu | DNP-Gly | DNP-Leu | ε-DNP-Lys |
|  |  |  |  |  |
| DNP-Phe | DNP-Pro | DNP-Ser | DNP-Thr | DNP-Trp |
|  |  |  |  |  |
| DNP-Tyr | DNP-Val | 2-Carboxy-1-naphthol | p-Cresotic acid | Cycrimine |
|  |  |  |  | |
| Diaspirin | Hemimellitic acid | 2-Naphthylamine | α-Nitrolocinnamic acid | |
|  |  |  |  |  |
| Phenazopyridine | Proniumiodide | Acetazolamide | Furosemide | DNP-Met |

satisfactory QSAR analyses. Therefore, we used the results of docking experiments instead for aligning the molecules, a procedure that proved to be very successful.

Materials and Methods

Haptens. All antigens were taken into the analysis in the protonated state which is likely to prevail in solution under physiological and experimental conditions (pH 7.2). Cycrimine

is used as a racemic drug and, therefore, was tested as such. Since docking suggested that both enantiomers bind well, they were treated identically, assuming that the separate association constants do not differ significantly from the measured mean value.

Association Constants. Association constants were obtained from studies by Varga *et al.*⁹ Association was assessed by UV-vis-spectroscopy,¹⁸ using mAbs isolated and purified



Figure 1. Alignment of the ligands using a hydrogen-devoid backbone-type representation.

from tissue culture media by affinity chromatography. The error in the measurement of the binding constants was below 5%. For the CoMFA, the logarithm of the association constants was used, thus correlating the data linearly to the binding energies.

Modeling. Docking of the haptens was performed using a modified version of AUTODOCK,¹¹ as described earlier.¹⁰ The program AUTODOCK uses a Metropolis Monte Carlo algorithm of simulated annealing for positional and conformational searching. This is done in combination with a rapid energy evaluation through precalculated grids of molecular affinity potentials which allow the inclusion of van der Waals, electrostatic, and hydrogen-bonding interactions. During the docking process, the conformational space of the ligand is controlled through user-defined restraints. For most of the 27 antigens examined, several reasonable binding orientations/conformations were obtained. Therefore, in order to derive a consistent QSAR model from these geometries, the following strategy was applied: As a starting set, nine ligands were defined which had either two or three distinct final docked orientations in the 10 docking runs. The possible alignments were subjected to the CoMFA procedure, and the alignment was chosen which gave the best r^2_{cv} value. The remaining haptens were then added successively by choosing that orientation which gave the best model with respect to r^2_{cv} . The ligand orientation with the smallest residual was chosen because the calculated energies do not comprise entropic contributions. Therefore the residual was used as a guideline to find the best "entropy-corrected" orientation, which was then included in the model. Alignments which gave rise to only slightly worse r^2_{cv} values were not discarded but investigated in combination with newly added haptens. In these cases, the alignment most consistent with the relative orientation of other antigens was selected. The alignment of the molecules investigated is visualized in Figure 1. It is evident that the molecules binding to the tight pocket are more confined in space, whereas the other molecules show more variation in their relative orientation.

The CoMFAs were performed using SYBYL 6.0¹⁹ on IBM RS6000/550 and Silicon Graphics workstations. Partial atomic charges of the haptens were calculated using the semiempirical method AM1²⁰ implemented in MOPAC 6.0.²¹

The CoMFA grid extended the superimposed molecules by 4 Å in all directions of a Cartesian coordinate system. The noncovalent (steric and electrostatic) potential energy fields of each molecule were calculated using the Lennard-Jones and Coulombic potential function of the Tripos force field.²² An sp^3 carbon with a probe charge of +1 served as a probe atom. A distance-dependent dielectric constant was applied, and the steric and electrostatic cutoff values were set to ± 30 kcal/mol. At lattice intersections "inside" the molecules (as determined by a corresponding steric interaction energy value of 30.0 kcal/mol) no electrostatic energies were calculated. The statistical findings were then compared to results obtained using a hydrogen atom (charge +1) as probe atom. Additional analyses were carried out using a grid of the same size and position, but a spacing of 1.0 Å. In order to investigate the sensitivity of the CoMFAs to the grid position, analyses with

Table 2. Summary of the CoMFA Results

| model | probe atom (charge) | grid spacing, Å | r^2_{cv} | k^a | r^2^b | steric contribution ^c |
|-------|------------------------|--------------------|------------|-------|---------|-------------------------------------|
| A | C sp^3 (+) | 2 | 0.785 | 5 | 0.974 | 0.467 |
| B | C sp^3 (+) | 1 | 0.773 | 5 | 0.972 | 0.498 |
| C | C sp^3 (+) | 2 | 0.809 | 6 | 0.994 | 0.513 |
| D | H (+) | 2 | 0.773 | 6 | 0.991 | 0.468 |

^a Optimum number of components. ^b Conventional r^2 determined with this number of components. ^c The sum of steric and electrostatic contributions equals 1.0.

the region shifted along the three axes of a Cartesian coordinate system were performed as well. In order to assess the necessity of using both steric and electrostatic fields, analyses using just one of the two field types were carried out.

The regression equations were derived by means of the PLS algorithm,^{13–15} as implemented in SYBYL 6.0. The latent variables were subjected to the leave-one-out cross-validation test in order to evaluate the number of components yielding the highest r^2_{cv} . The standard deviation threshold (minimum σ) was set to 2.0.

Results and Discussion

The best CoMFA using an sp^3 carbon as a probe atom (model A, Tables 2 and 3) has an r^2_{cv} of 0.785. The underlying alignment for this model contained only one orientation out of several possible ones for each hapten. Therefore, the question was raised whether the high consistency of this QSAR model was an artefact in that sense that the alignment of each compound was chosen with respect to a constant grid definition. In order to address this question, several analyses with altered grids were carried out: At first, the spacing of the lattice intersections was reduced to 1.0 Å. The resulting model had a slightly reduced r^2_{cv} (0.773, model B). This was in fact no surprise, since it has been observed more often that a finer grid does not lead to an improvement of the results.^{12,23} Such a phenomenon can be ascribed to an unproportional increase of noise in the calculated interaction energies.²⁴ In subsequent analyses, the grid was shifted by ± 0.5 and ± 1.0 Å relative to its original position (Table 4). The results indicated that the quality of the QSAR models were almost independent from the grid positions chosen; in some cases the predictiveness of the analyses even increased slightly. The best model yielded an r^2_{cv} of 0.809 at a grid offset of -1.0 Å in the y -direction and is referred to as model C.

In addition to the grid variations, an analysis was carried out using a proton as the probe atom. This was done in order to obtain an estimate of the importance of hydrogen bonding in the ligand–receptor interactions. The corresponding r^2_{cv} (0.773, model D) was of similar magnitude as the other models.

The importance of using both steric and electrostatic fields was clearly demonstrated by comparing the r^2_{cv} values of the analyses using both field types with the CoMFAs using one descriptor type only. For model C, the r^2_{cv} using only steric fields reduced to 0.597 (both, 0.809), using the electrostatic fields alone yielded an r^2_{cv} of 0.318. Similar values were obtained for analysis D (steric only, 0.577; electrostatic only, 0.581; both, 0.773), indicating the importance of both field types for an adequate description of the molecules.

A very useful result of the CoMFA procedure are the so-called "standard deviation * coefficient plots". These plots indicate those regions where putative substituents have a high influence on binding. In the following

Table 3. Measured and Predicted log K_A Values

| hapten | measured activity | model A | | model C | | model D | |
|-------------------------|-------------------|--------------------|----------|--------------------|----------|--------------------|----------|
| | | predicted activity | residual | predicted activity | residual | predicted activity | residual |
| carboxynaphthol | 6.708 | 6.420 | 0.288 | 6.626 | 0.082 | 6.576 | 0.132 |
| phenazopyridine | 6.497 | 6.463 | 0.034 | 6.478 | 0.019 | 6.480 | 0.017 |
| DNP-Val | 5.931 | 6.001 | -0.070 | 5.946 | -0.015 | 6.003 | -0.072 |
| DNP-Trp | 5.929 | 5.919 | 0.010 | 5.906 | 0.023 | 5.895 | 0.034 |
| DNP-Ala | 5.796 | 5.898 | -0.102 | 5.820 | -0.024 | 5.860 | -0.064 |
| DNP-Phe | 5.783 | 5.874 | -0.091 | 5.829 | -0.046 | 5.867 | -0.084 |
| naphthylamine | 5.713 | 5.705 | 0.008 | 5.768 | -0.055 | 5.732 | -0.019 |
| DNP-Ser | 5.504 | 5.498 | 0.006 | 5.484 | 0.020 | 5.491 | 0.013 |
| DNP-Asp | 5.496 | 5.487 | 0.009 | 5.503 | -0.007 | 5.514 | -0.018 |
| DNP-Thr | 5.491 | 5.515 | -0.024 | 5.474 | 0.017 | 5.452 | 0.039 |
| DNP-Leu | 5.394 | 5.368 | 0.026 | 5.402 | -0.008 | 5.336 | 0.058 |
| <i>p</i> -cresylic acid | 5.384 | 5.573 | -0.189 | 5.485 | -0.101 | 5.471 | -0.087 |
| DNP-Pro | 5.190 | 5.184 | 0.006 | 5.203 | -0.013 | 5.197 | -0.007 |
| DNP-Gln | 5.079 | 5.154 | -0.075 | 5.143 | -0.064 | 5.171 | -0.092 |
| DNP-Arg | 5.041 | 5.108 | -0.067 | 5.040 | 0.001 | 5.066 | -0.025 |
| cyano-cinnamic acid | 5.041 | 5.023 | 0.018 | 4.967 | 0.074 | 5.029 | 0.012 |
| DNP-Asn | 4.919 | 4.800 | 0.119 | 4.940 | -0.021 | 4.870 | 0.049 |
| DNP-Gly | 4.903 | 4.704 | 0.199 | 4.872 | 0.031 | 4.886 | 0.017 |
| DNP | 4.886 | 4.965 | -0.079 | 4.914 | -0.028 | 4.81 | 0.005 |
| DNP-Tyr | 4.851 | 4.875 | -0.024 | 4.761 | 0.090 | 4.774 | 0.077 |
| cycrimine R | 4.839 | 4.883 | -0.044 | 4.824 | 0.015 | 4.800 | 0.039 |
| cycrimine S | 4.839 | 4.856 | -0.017 | 4.762 | 0.077 | 4.788 | 0.051 |
| hemimellitic acid | 4.771 | 4.756 | 0.015 | 4.751 | 0.021 | 4.758 | 0.013 |
| prolonium iodide | 4.663 | 4.647 | 0.016 | 4.709 | -0.046 | 4.726 | -0.063 |
| DNP-Glu | 4.633 | 4.642 | -0.009 | 4.625 | 0.008 | 4.604 | 0.029 |
| diaspirin | 4.568 | 4.606 | -0.038 | 4.595 | -0.027 | 4.625 | -0.057 |
| DNP-Lys | 4.380 | 4.305 | 0.075 | 4.401 | -0.021 | 4.376 | 0.004 |

Table 4. Influence of Different Grid Offsets on the CoMFAs

| offset (Å) | x-axis | | | | y-axis | | | | z-axis | | | |
|------------|--------|-------|-------|-------|--------|-------|-------|-------|--------|-------|-------|-------|
| | +0.5 | -0.5 | +1.0 | -1.0 | +0.5 | -0.5 | +1.0 | -1.0 | +0.5 | -0.5 | +1.0 | -1.0 |
| r^2_{cv} | 0.756 | 0.764 | 0.744 | 0.743 | 0.749 | 0.802 | 0.809 | 0.809 | 0.737 | 0.802 | 0.772 | 0.772 |
| k^a | 5 | 5 | 5 | 5 | 5 | 6 | 6 | 6 | 5 | 6 | 5 | 5 |

^a Optimum number of components.

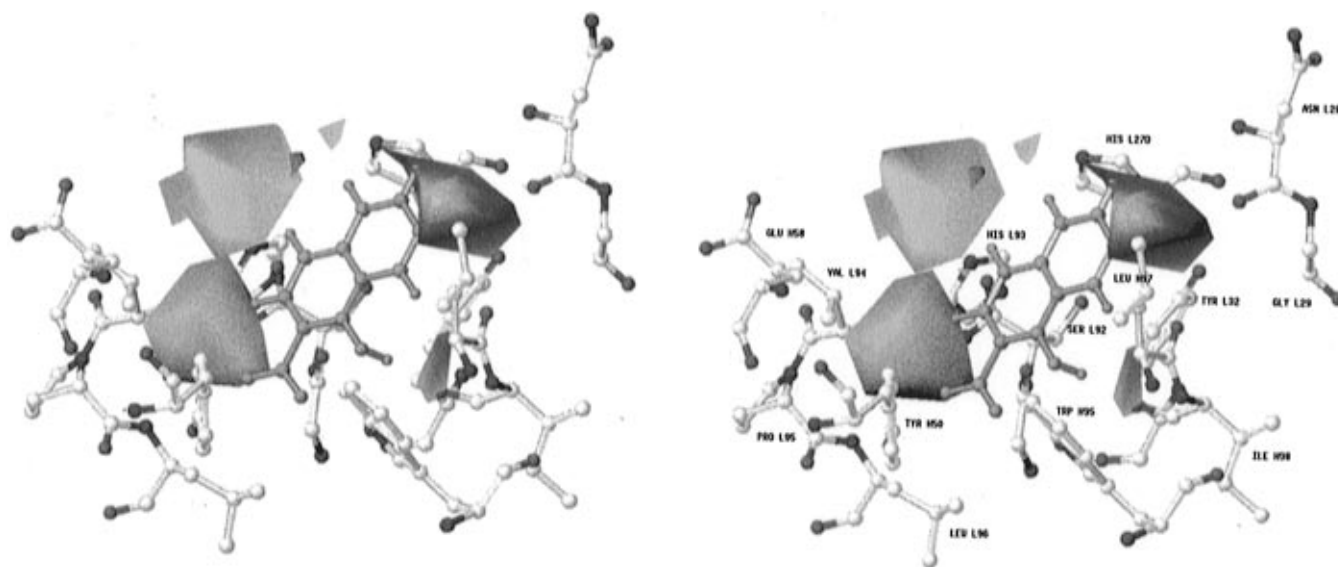


Figure 2. Stereoview of the CoMFA contour map (standard deviation * coefficients) for analysis C. Green contours indicate regions where steric interactions with the receptor increase binding; in the yellow areas steric interactions are least important. 2-Carboxy-1-naphthol (colored green) is shown as a reference.

paragraphs, the QSAR models will be discussed with respect to these contour plots.

The analyses performed with an sp^3 carbon (A through C) gave very similar coefficient contour maps. As model C yielded the highest r^2_{cv} in this series, it was chosen for further interpretation. In the binding site on the protein, which is formed by a pit with a small side pocket, two areas could be detected where steric inter-

action with the receptor should lead to a higher binding affinity (Figure 2). The bigger area is located in the vicinity of the amino acids His L 27D, Asn L 28, Gly L 29, Tyr L 32, and Leu H 97 and can be explained by strong van der Waals interactions that sterically bulky substituents of antigens can form with His L 27D, Tyr L 32, and Leu H 97. For the same reason a substituent near Leu H 97, Ile H 98, and Trp H 95 contributes

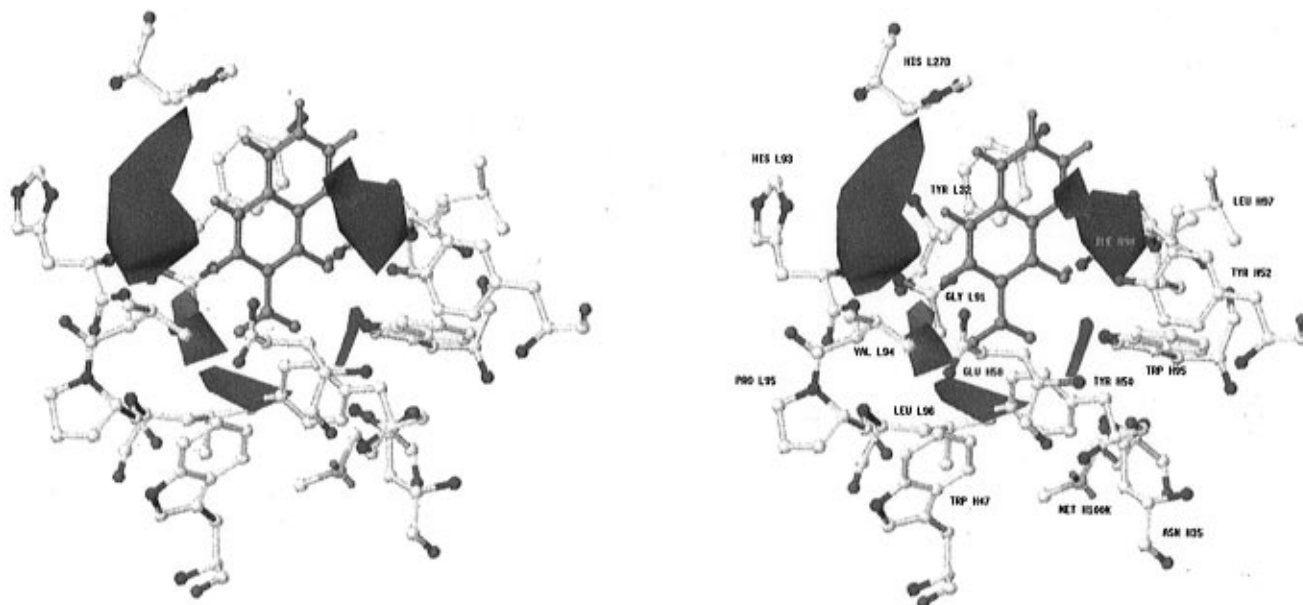


Figure 3. Stereoview of the CoMFA contour map (standard deviation * coefficients) for analysis C. Areas where positively charged substituents are favored are colored blue; regions where negatively charged substituents should bind preferably are colored red. 2-Carboxy-1-naphthol (colored green) is shown as a reference.

advantageously to the binding energy (small green region in Figure 2).

An area where bulky substituents of the haptens appear to cause unfavorable interactions with the receptor is surrounded by amino acids Gly L91, Ser L92, His L93, and Val L94 of the light chain and Trp H47, Tyr H50, and Glu H58 of the heavy chain. At first sight it appears somewhat puzzling that there are areas of seemingly unfavorable steric interactions, since the alignment has been generated by docking, implying that there are only few bad contacts between the individual molecules and the receptor. However, for an interpretation of this data one should bear in mind that the compounds were docked to a rigid receptor structure. Therefore, it appears possible that the area of unfavorable steric interaction actually indicates the requirement for higher receptor flexibility particularly in this region for an optimum accommodation of ligand molecules.

The bottom of the binding site is formed by the amino acids Gly L91, Val L94, Pro L95, Leu L96, Asn H35, Trp H47, Trp H95, and Met H100K surrounding Tyr H50. According to the electrostatic coefficient contour map (Figure 3), compounds bearing negatively charged substituents are able to form favorable interactions with the residues in this region. This could be ascribed to the formation of hydrogen bonds with the OH group of Tyr H50. A second area of favorable interaction between negatively charged parts of haptens and the receptor is located near Tyr H52. Also in this case, binding appears to be increased by hydrogen bond formation.

Two areas where positively charged ligands/substituents should bind preferably to the receptor can be identified in analysis C. The first one is surrounded by the side chains of His L27D, Tyr L32, Ser L92, and His L93. In case of the latter two residues, the backbone oxygens appear to be involved in such an interaction. The second area is located in the vicinity of Trp H95, Leu H97, and Ile H98. Also in this region,

backbone oxygens (of Leu H97 and Ile H98) contribute to the binding of ligands with positively charged substituents.

Upon comparison of the coefficient contour maps of models C and D (the latter being derived with a hydrogen as probe atom), only minor differences become apparent. The steric coefficient contour map of analysis D (Figure 4) is virtually identical with that of analysis C. The most significant difference can be found in the electrostatic contours for analysis D (Figure 5). The area for favorable interaction of a positively charged substituent with the receptor near Ile H98 extends further down to the bottom of the binding site. In particular the backbone oxygen of Phe H99 appears to be responsible for this feature.

The best test for the general validity of a QSAR analysis is to predict the activity of molecules which were not members of the training set. In the present study, this was done for three additional compounds (Table 5). Compared to the training set, these haptens are unique because they contain sulfur atoms. Since the version of AUTODOCK used in this study did not contain parameters for sulfur, these haptens were docked manually to the antibody. The most similar compounds in the training set served as templates. Despite the fact that the new haptens were unique compared to the training set, all CoMFA models were able to predict the activities of these molecules rather accurately, indicating a high predictiveness of the analyses. In order to quantify the quality of the predictions, we compared the root-mean-square errors in the training and test sets of models C and D. For both models the error for the test set was found to be of similar magnitude than the one for the training set (root-mean-square error for model C, training set = 0.249, test set = 0.200; for model D, training set = 0.272, test set = 0.236), demonstrating the quality of the predictions.

As the models were the result of a novel alignment procedure, in some cases involving the selection of a particular orientation for a given molecule, we were

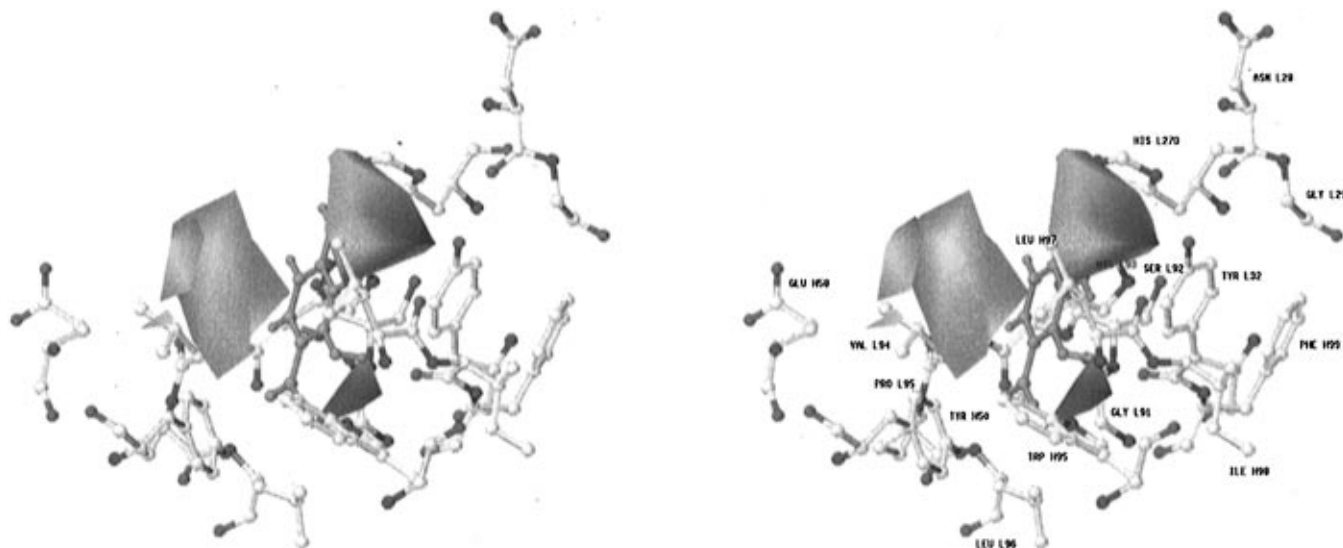


Figure 4. Stereoview of the CoMFA contour map (standard deviation * coefficients) for analysis D. Green contours indicate regions where steric interactions with the receptor increase binding; in the yellow areas steric interactions are least important. 2-Carboxy-1-naphthol (colored green) is shown as a reference.

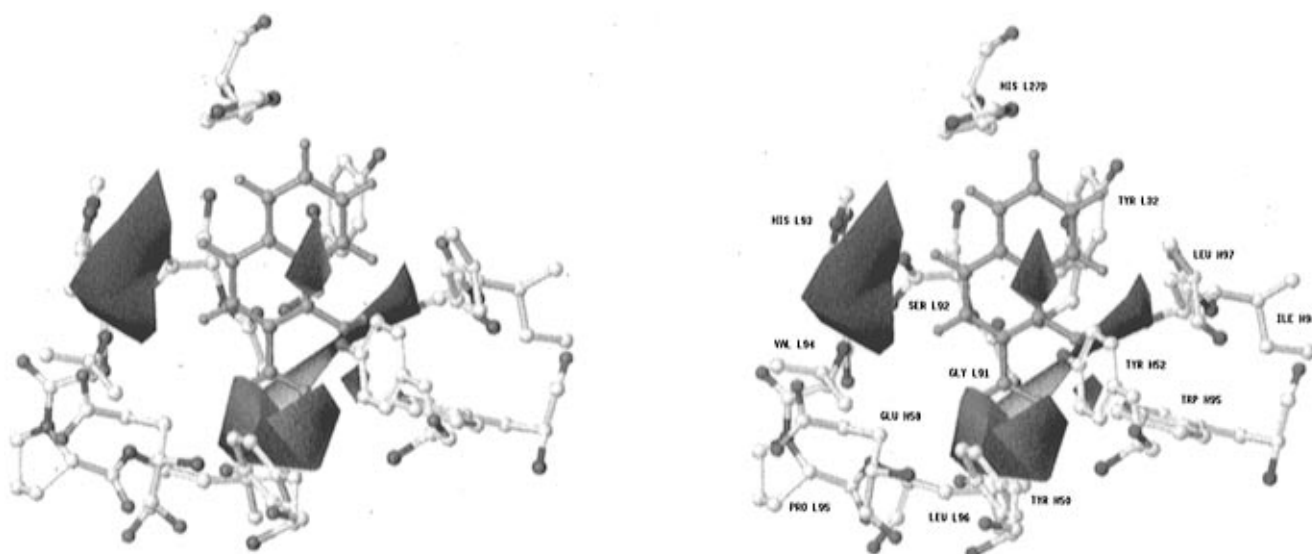


Figure 5. Stereoview of the CoMFA contour map (standard deviation * coefficients) for analysis D. Areas where positively charged substituents are favored are colored blue; regions where negatively charged substituents should bind preferably are colored red. 2-Carboxy-1-naphthol (colored green) is shown as a reference.

Table 5. Predicted and Measured log K_A Values of Sulfur-Containing Haptens

| hapten ^a | predicted activity | | measured activity |
|---------------------|--------------------|---------|-------------------|
| | model C | model D | |
| acetazolamide | 4.96 | 4.81 | 5.00 |
| furosemide | 5.44 | 5.50 | 5.27 |
| DNP-Met | 6.02 | 6.00 | 5.72 |

^a The trade names for acetazolamide and furosemide are Diamox and Lasix, respectively.

interested in assessing the likelihood of chance correlation. Therefore, the activities in models C and D were randomized 100 times, i.e. 100 activity columns with randomly interchanged activity values were generated. The resulting 100 CoMFAs indicated that the likelihood for chance correlation is very low. The mean r^2_{cv} for C was found to be -0.221 (standard deviation, 0.252), while for D the mean was -0.186 (standard deviation, 0.250).

Conclusions

Thus far, CoMFA has been carried out on data sets containing rather similar compounds (for some recent studies see refs 25–29). For such data sets, alignment procedures based on a common, previously derived, pharmacophore or based on methods such as the “active analogue approach” have proven very successful. However, the molecules investigated in the present study displayed such a high dissimilarity that a pharmacophore-based alignment approach had to fail. Therefore, we applied a novel strategy and aligned the haptens by docking them to a receptor structure using the program AUTODOCK. The quality of the QSAR models showed that the combination of automated docking and CoMFA could be very useful, in particular for very diverse data sets. Other approaches to perform “receptor-based” alignments appeared in the literature.³⁰ Waller et al. used crystallographic data for the determination of alignment rules followed by field-fit minimization as a molecular superimposition tool. However, so far no one

has simulated the entire docking process and used the final orientations/conformations for the alignment.

The CoMFA models indicated that several amino acids of the receptor might be crucial for binding of the haptens. A feature of particular interest shown by the QSARs was the strong participation of aromatic side chains in binding of the antigens to the immunoglobulins. These residues have been postulated previously to be important for binding and to account for the multispecificity of antibodies.³¹ The explanation given was that tyrosine and tryptophan have amphipathic properties which allow them to undergo readily the change from a hydrophilic to a lipophilic environment, a process which occurs during binding. Furthermore, these residues are able to form favorable van der Waals and electrostatic interactions with a variety of antigens. Some degree of flexibility in the side chains of these amino acids will help to accommodate haptens via an induced-fit process. The importance of the amino acids Tyr H 52, Tyr H 50, and Trp H 95 as hydrogen bond donors and His L 27D, Tyr L 32, and Trp H 95 for interaction with positively charged ligands/substituents has been claimed earlier, and the present results give further support for this hypothesis.

Acknowledgment. This work was supported by a grant (No. P10229-MED) from the Austrian Research Council.

References

- Talmage, D. W. Immunological specificity. *Science* **1959**, *129*, 1643–1645.
- Richards, F. F.; Konigsberg, W. H.; Rosenstein, R. W.; Varga, J. M. On the specificity of antibodies: biochemical and biophysical evidence indicates the existence of polyfunctional antibody combining regions. *Science* **1975**, *187*, 130–137.
- Varga, J. M.; Konigsberg, W. H.; Richards, F. F. Antibodies with multiple binding functions. Induction of single immunoglobulin species by structurally dissimilar haptens. *Proc. Natl. Acad. Sci. U.S.A.* **1973**, *70*, 3269–3274.
- Imanishi, T.; Makela, O. Inheritance of antibody specificity - I. Anti-(4-hydroxy-3-nitrophenyl)acetyl of the mouse primary response. *J. Exp. Med.* **1974**, *140*, 1498–1510.
- Rudolph, A. K.; Burrows, P. D.; Wahl, M. R. Thirteen hybridomas secreting hapten-specific immunoglobulin E from mice with Iga and Igb heavy chain haplotype. *Eur. J. Immunol.* **1981**, *11*, 527–529.
- Furusawa, S.; Ovary, Z. Heteroclitic antibodies: difference in fine specificity between monoclonal antibodies directed against dinitrophenyl and trinitrophenyl hapten. *Int. Arch. Allergy Appl. Immunol.* **1988**, *85*, 238–243.
- Varga, J. M.; Kalchschmid, G.; Klein, G.; Fritsch, P. Mechanism of allergic cross-reactions - I. Multispecific binding of ligands to a mouse monoclonal anti-DNP IgE antibody. *Mol. Immunol.* **1991**, *28*, 641–654.
- Kofler, H.; Schnegg, I.; Geley, S.; Helmsberg, A.; Varga, J. M.; Kofler, R. Mechanism of allergic cross-reactions - III. cDNA cloning and variable region sequence analysis of two IgE antibodies specific for trinitrophenyl. *Mol. Immunol.* **1992**, *29*, 161–166.
- Droupadi, P. R.; Varga, J. M.; Linthicum, D. S. Mechanism of allergenic cross-reactions - IV. Evidence for participation of aromatic residues in the ligand binding site of two multi-specific IgE monoclonal antibodies. *Mol. Immunol.* **1994**, *31*, 537–548.
- Winger, R. H.; Liedl, K. R.; Sotriffer, C. A.; Gamper, A. H.; Kroemer, R. T.; Rode, B. M.; Varga, J. M. Prediction of antibody-ligand complex structures by automated docking - Binding of small molecules to a mouse monoclonal IgE antibody. *J. Mol. Recognit.*, in press.
- Goodsell, D. S.; Olson, A. J. Automated Docking of Substrates to Proteins by Simulated Annealing. *PROTEINS: Struct. Funct. Genet.* **1990**, *8*, 195–202.
- Cramer, R. D. III; Patterson, D. E.; Bunce, J. D. Comparative Molecular Field Analysis (CoMFA). 1. Effect of Shape on Binding of Steroids to Carrier Proteins. *J. Am. Chem. Soc.* **1988**, *110*, 5959–5967.
- Wold, S.; Albano, C.; Dunn W. J.; Edlund, U.; Esbenson, K.; Geladi, P.; Hellberg, S.; Lindberg, W.; Sjöström, M. In *Chemometrics: Mathematics and Statistics in Chemistry*; Kowalski, B., Ed.; Reidel: Dordrecht, The Netherlands, 1984; pp 17–95.
- Dunn, W. J.; Wold, S.; Edlund, U.; Hellberg, S.; Gasteiger, J. Multivariate Structure-Activity Relationship Between Data from a Battery of Biological Tests and an Ensemble of Structure Descriptors: The PLS Method. *Quant. Struct.-Act. Relat.* **1984**, *3*, 131–137.
- Geladi, P. Notes on the History and Nature of Partial Least Squares (PLS) Modelling. *J. Chemomet.* **1988**, *2*, 231–246.
- Cramer, R. D., III; Bunce, J. D.; Patterson, D. E. Crossvalidation, Bootstrapping and Partial Least Squares Compared with Multiple Regression in Conventional QSAR Studies. *Quant. Struct.-Act. Relat.* **1988**, *7*, 18–25.
- Marshall, G. R.; Barry, C. D.; Bosshard, H. E.; Dammkoehler, R. A.; Dunn, D. A. The conformational parameters in drug design. In *Computer-Assisted Drug Design*; Olson, E. C., Christoffersen, R. E., Eds.; ACS Symp. Series No. 112, American Chemical Society: Washington, DC, 1979; pp 205–226.
- Droupadi, P. R.; Anchim, J. M.; Meyers, E. A.; Linthicum, D. S. Spectrofluorometric study of the intermolecular complexation of monoclonal antibodies with the high potency sweetener N-(p-cyanophenyl)-N'-(diphenylmethyl)guanidineacetic acid. *J. Mol. Recognit.* **1993**, *5*, 173–179.
- The program SYBYL 6.0 is available from Tripos Assoc., 1699 S. Hanley Rd., St. Louis, MO 63144.
- Dewar, M. J. S.; Zoebisch, E. G.; Healy, E. F.; Stewart, J. J. P. AM1: A New General Purpose Quantum Chemical Mechanical Molecular Model. *J. Am. Chem. Soc.* **1985**, *107*, 3902–3909.
- The program MOPAC 6.0 is available from Quantum Chemistry Program Exchange No. 455.
- Clark, M.; Cramer, R. D., III; Van Opdenbosch, N. Validation of the general purpose Tripos 5.2 force field. *J. Comput. Chem.* **1989**, *10*, 982–1012.
- Kroemer, R. T.; Hecht, P. Replacement of steric 6-12 potential-derived interaction energies by atom-based indicator variables in CoMFA leads to models of higher consistency. *J. Comput.-Aided Mol. Design.* **1995**, *9*, 205–212.
- Clark, M.; Cramer, R. D. III. The probability of chance correlation using Partial Least Squares (PLS). *Quant. Struct.-Act. Relat.* **1993**, *12*, 137–145.
- Debnath, A. K.; Jiang, S.; Strick, N.; Lin, K.; Haberfield, P.; Neurath, A. R. Three-Dimensional Structure-Activity Analysis of a Series of Porphyrin Derivatives with Anti-HIV-1 Activity Targeted to the V3 Loop of the gp120 Envelope Glycoprotein of the Human Immunodeficiency Virus Type 1. *J. Med. Chem.* **1994**, *37*, 1099–1108.
- Avery, M. A.; Gao, F.; Chong W. K. M.; Mehrotra S.; Milhous, W. K. Structure-Activity Relationships of the Antimalarial Agent Artemisinin. 1. Synthesis and Comparative Molecular Field Analysis of C-9 Analogs of Artemisinin and 10-Deoxoartemisinin. *J. Med. Chem.* **1993**, *36*, 4264–4275.
- Carroll, F. I.; Mascarella, S. W.; Kuzemko, M. A.; Gao, Y.; Abraham, P.; Lewin, A. H.; Boja, J. W.; Kuhar, M. J. Synthesis, Ligand Binding, and QSAR (CoMFA and Classical) Study of 3β-(3'-Substituted phenyl)-, 3β-(4'-Substituted phenyl)-, and 3β-(3',4'-Disubstituted phenyl)tropane-2β-carboxylic Acid Methyl Esters. *J. Med. Chem.* **1994**, *37*, 2865–2873.
- Tong, W.; Collantes, E. R.; Chen, Y.; Welsh, W. J. A Comparative Molecular-Field Analysis Study of N-Benzylpiperidines as Acetylcholinesterase Inhibitors. *J. Med. Chem.* **1996**, *39*, 380–387.
- Kroemer, R. T.; Ettmayer, P.; Hecht, P. 3D-Quantitative Structure-Activity Relationships of Human Immunodeficiency Virus Type-1 Proteinase Inhibitors: Comparative Molecular Field Analysis of 2-Heterosubstituted Statine Derivatives—Implications for the Design of Novel Inhibitors. *J. Med. Chem.* **1995**, *38*, 4917–4928.
- Waller, C. L.; Oprea, T. I.; Giolitti, A.; Marshall, G. R. Three-Dimensional QSAR of Human Immunodeficiency Virus (I) Protease Inhibitors. 1. A CoMFA Study Employing Experimentally-Determined Alignment Rules. *J. Med. Chem.* **1993**, *36*, 4152–4160.
- Mian, I. S.; Bradwell, A. R.; Olson, A. J. Structure, Function and Properties of Antibody-Binding Sites. *J. Mol. Biol.* **1991**, *217*, 133–151.

JM960229I